Supplement of Hydrol. Earth Syst. Sci., 24, 115–142, 2020
https://doi.org/10.5194/hess-24-115-2020-supplement

Hydrology and Earth System Sciences
Open Access
EGU

Supplement of

Stream temperature and discharge evolution in Switzerland over the last 50 years: annual and seasonal behaviour

Adrien Michel et al.

Correspondence to: Adrien Michel (adrien.michel@epfl.ch)

Supplement

Abstract. The present supplementary material is complementing the key elements of the study presented in the main part of this work. It either expands on results which were too voluminous for the main article or gives elements for a better understanding and potential reproduction of the results. Often, the article only shows pertinent examples while the larger body of corresponding results is included here. The first part is a collection of tables and figures related to the data and methods presented (Section S1), followed by additional figures and tables detailing and complementing the main results in the article (Section S2). All descriptions and explanations necessary to understand the material below, as well as all the general conclusions, are provided in the text of the paper. The availability of the data and code are also mentioned and discussed in the article.

S1 Supplementary materials about data and methods

S1.1 Excluded catchments

Some catchments have been excluded from the analysis for various reasons. They are listed below in Table S1.

Table S1. River measurement stations removed from the study and justifications. The hydrological regimes are Swiss Plateau and Jura regime (SPJ), Alpine regime (ALP), and Downstream lake regime (DLA). The data providers are the Swiss Federal Office for the Environment (FOEN) and the Office for water and waste of the Canton of Bern (AWA).

River	Temperature measurement	Discharge measurement	Hydrological regime	Data provider	Reason for removal
Foul in Moutier	1995-2018	1995-2018	SPJ	AWA	Issues in temperature values (no annual cycle)
Birse in Court, Pont de la STEP	1996-2018	1996-2018	SPJ	AWA	Downstream a wastewater treatment plant
Louibach in Gstaad, Badweidli	1995-2018	1994-2018	ALP	AWA	1.5 year gap in water temperature, temperature only every 2 hours before 2000
Suze in Péry, Vigier Ciment	1996-2018	1992-2018	SPJ	AWA	Disturbance because of a cement factory
Urtenen in Kernenried	1997-2018	1997-2018	SPJ	AWA	Downstream a wastewater treatment plant
Chalière in Moutier, Pont de la STEP	1997-2018	1997-2018	SPJ	AWA	1.5 year gap in water temperature
Entschlige in Frutigen, Tropenhaus	1998-2018	1998-2018	ALP	AWA	Multiple gaps in the time series
Rhein in Weil, Palmrainbrücke	1995-2018	1992-2018	DLA	FOEN	Data only since 1995, already many stations on the Rhein River

S1.2 MeteoSwiss stations details

Table S2 summarizes information about the MeteoSwiss stations used.

Table S2. Details of MeteoSwiss stations used including the periods for air temperature, precipitation, homogeneous air temperature and homogeneous precipitation time series. Coordinates are indicated in CH1903 coordinate system.

Station name	Station abbreviation	Easting coordinates	Northing coordinates	Station elevation measurement	Air temp. measurement	Hom. air temp. measurement	Precipitation measurement	Hom. precipitation
Adelboden	ABO	609350	149001	1322	1959-2018	-	1950-2018	-
Altdorf	ALT	690180	193564	438	1950-2018	1950-2018	1950-2018	1950-2018
Basel-Binningen	BAS	610908	265611	316	1950-2018	1950-2018	1950-2018	1950-2018
Passo-del-Bernina	BEH	798422	143020	2260	1972-2018	-	1950-2018	-
Bern-Zollikofen	BER	601933	204409	552	1950-2018	1950-2018	1950-2018	1950-2018
La-Chaux-de-Fonds	CDF	550919	214861	1017	1950-2018	1950-2018	1950-2018	1950-2018
Chasseral	CHA	570845	220157	1599	1981-2018	-	1981-2018	-
Chur	CHU	759465	193152	556	1950-2018	-	1950-2018	-
Delémont	DEM	593269	244543	439	1959-2018	-	1950-2018	-
Einsiedeln	EIN	699982	221068	910	1950-2018	-	1950-2018	-
Elm	ELM	732265	198425	957	1950-2018	1950-2018	1950-2018	1950-2018
Engelberg	ENG	674160	186069	1035	1950-2018	1950-2018	1950-2018	1950-2018
Glarus	GLA	723755	210567	516	1950-2018	-	1950-2018	-
Grächen	GRC	630738	116062	1605	1950-2018	1950-2018	1950-2018	1950-2018
Grimsel-Hospiz	GRH	668583	158215	1980	1950-2018	1950-2018	1950-2018	1950-2018
Col-du-Grand-St-Bernard	GSB	579192	79753	2472	1950-2018	1950-2018	1950-2018	-
Genève-Cointrin	GVE	498904	122631	410	1954-2018	1954-2018	1950-2018	1954-2018
Hallau	HLL	677456	283472	419	1959-2018	-	1950-2018	-
Interlaken	INT	633023	169092	577	1950-2018	-	1950-2018	-
Zurich-Kloten	KLO	682710	259338	426	1950-2018	-	1950-2018	-
Koppigen	KOP	612662	218664	485	1961-2018	-	1961-2018	-
Langnau-i.E.	LAG	628003	198793	743	1950-2018	-	1950-2018	-
Luzern	LUZ	665543	209849	454	1950-2018	1950-2018	1950-2018	1950-2018
Meiringen	MER	655844	175930	588	1950-2018	1950-2018	1950-2018	1950-2018
Mühleberg	MUB	587792	202479	479	1988-2018	-	1988-2018	-
Napf	NAP	638136	206078	1403	1978-2018	-	1978-2018	-
Neuchâtel	NEU	563086	205559	485	1950-2018	-	1950-2018	-
Locarno-Monti	OTL	704172	114342	366	1950-2018	1950-2018	1950-2018	1950-2018
Payerne	PAY	562131	184611	490	1965-2018	-	1965-2018	-
Bad-Ragaz	RAG	756910	209350	496	1950-2018	1950-2018	1950-2018	-
Santis	SAE	744183	234918	2502	1950-2018	-	1950-2018	1950-2018
Samedan	SAM	787249	155685	1708	1979-2018	-	1980-2018	1979-2018
S.Bernardino	SBE	734115	147294	1638	1968-2018	1968-2018	1968-2018	1968-2018
Segl-Maria IA	SIA	778574	144976	1804	1950-2018	-	1950-2018	1950-2018
Sion	SIO	591633	118583	482	1958-2018	1958-2018	1958-2018	1958-2018
Zurich-Fluntern	SMA	747865	254588	775	1866-2017	1866-2017	1890-2017	1866-2017
St.Gallen	STG	747865	254588	775	1950-2018	1950-2018	1950-2018	1950-2018
Aadorf-Tänikon	TAE	710517	259824	539	1971-2018	-	1970-2018	-
Vaduz	VAD	757722	221699	457	1971-2018	-	1971-2018	-
Wädenswil	WAE	693847	230744	485	1981-2018	-	1961-2018	-
Wynau	WYN	626404	233848	422	1978-2018	-	1978-2018	-

S1.3 STL analysis details

In this section, some examples of output of the STL analysis are presented. Figures S1 to S4 show the three different components of the STL (seasonal, trend, residuals) for the FOEN water station Reuss-Meillingen and for the MeteoSwiss station of Luzern. As we can see, the seasonal removal works correctly for water temperature, discharge, and air temperature. For precipitation, the effect is negligible. The STL method has been applied here with $n_s = 37$.

In Figures S5 and S6, the ACF and PACF of the residuals time series are shown (also with $n_s = 37$). If some seasonal signal still exists in the ACF, it is absent in the PACF, meaning that the data at one-year lag in time have no explanatory power on the current data, which is the goal to be achieved. In addition, this plot shows the absence of strong seasonality in the precipitation, especially, as we can expect, in the PACF, justifying the usage of these time series even if the STL has almost no effect.

Finally, in figures S7 and S8, the evolution of ACF and PACF for stream and air temperature residuals time series and for discharge and precipitation residuals time series for varying values of n_s are shown.

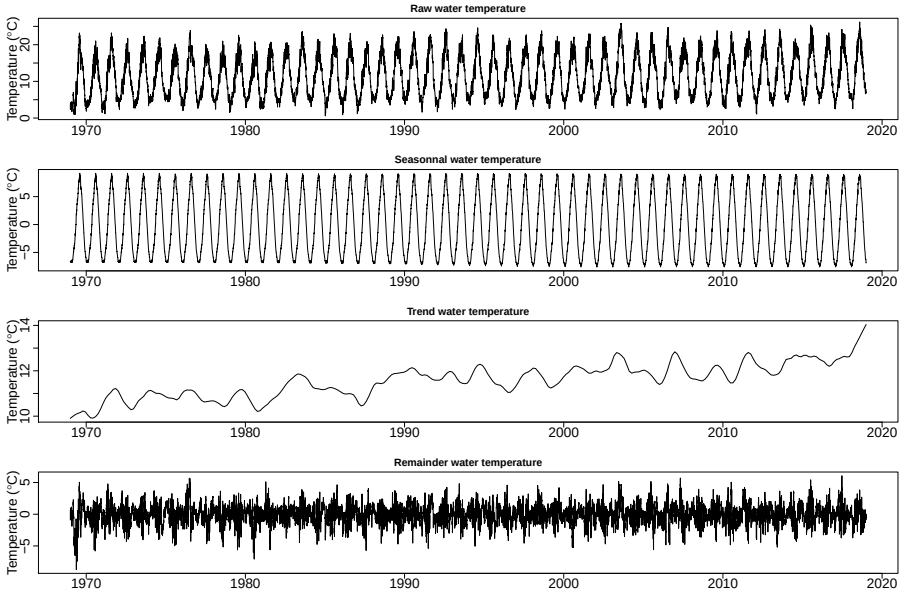

Figure S1. STL decomposition for water temperature for the Reuss River at the FOEN measurement station of Mellingen. Top: raw data, 2nd row: seasonal part, 3rd row: trend part, bottom: residuals. Series obtained with $n_s = 37$.

.

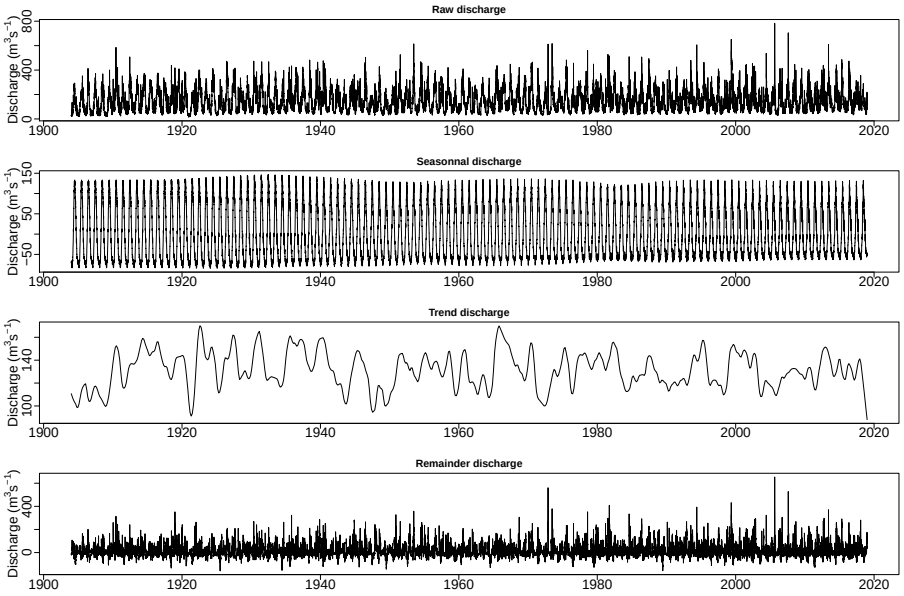

Figure S2. STL decomposition for discharge for the Reuss River at the FOEN measurement station of Mellingen. Top: raw data, 2[nd] row: seasonal part, 3[rd] row: trend part, bottom: residuals. Series obtained with $n_s = 37$.

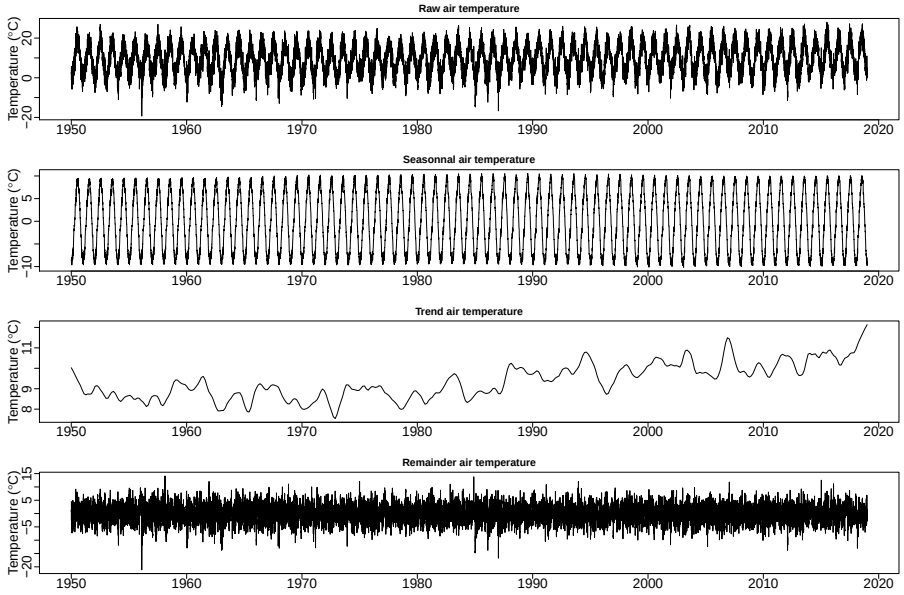

Figure S3. STL decomposition for air temperature for the MeteoSwiss measurement station of Luzern. Top: raw data, 2[nd] row: seasonal part, 3[rd] row: trend part, bottom: residuals. Series obtained with $n_s = 37$.

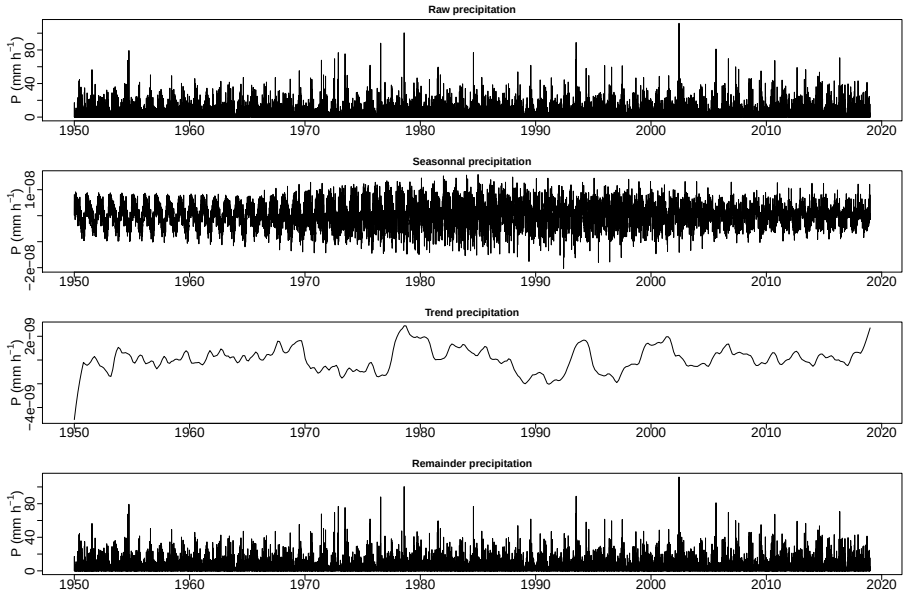

Figure S4. STL decomposition for precipitation for the MeteoSwiss measurement station of Luzern. Top: raw data, 2[nd] row: seasonal part, 3[rd] row: trend part, bottom: residuals. Series obtained with $n_s = 37$.

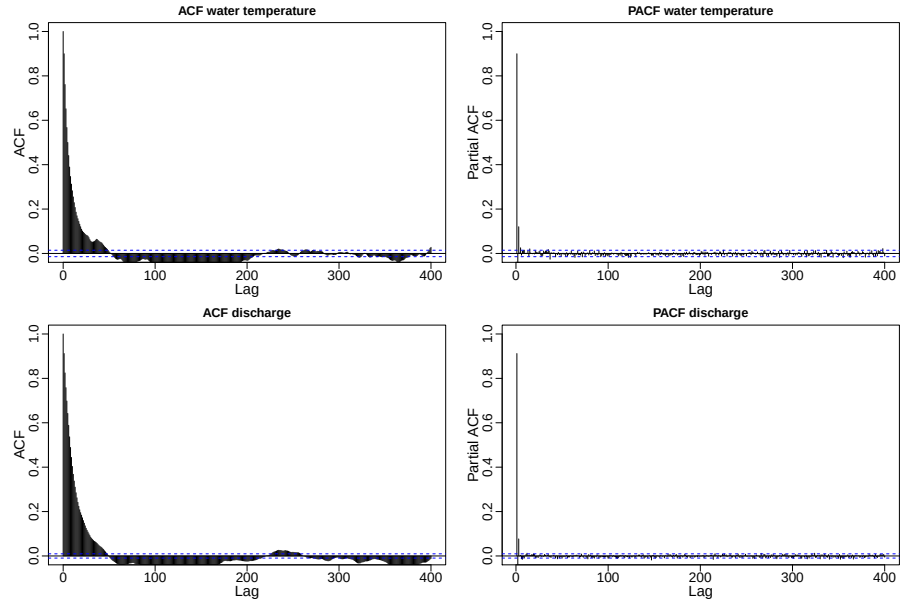

Figure S5. ACF and PACF of the residuals time series of the STL analysis for water temperature (top) and discharge (bottom) for the Reuss River at the FOEN measurement station of Mellingen.

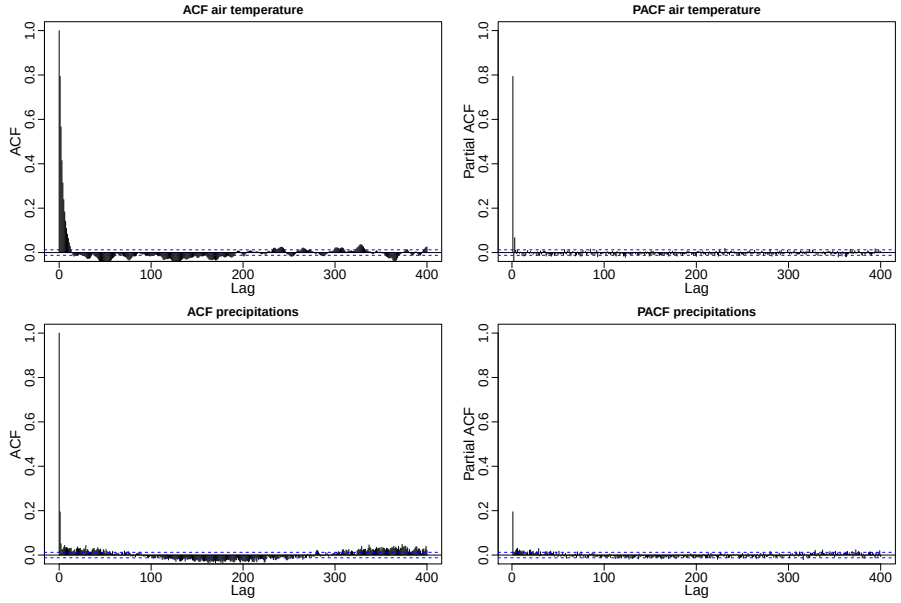

Figure S6. ACF and PACF of the residuals time series of the STL analysis for air temperature (top) and precipitation (bottom) for the MeteoSwiss measurement station of Luzern.

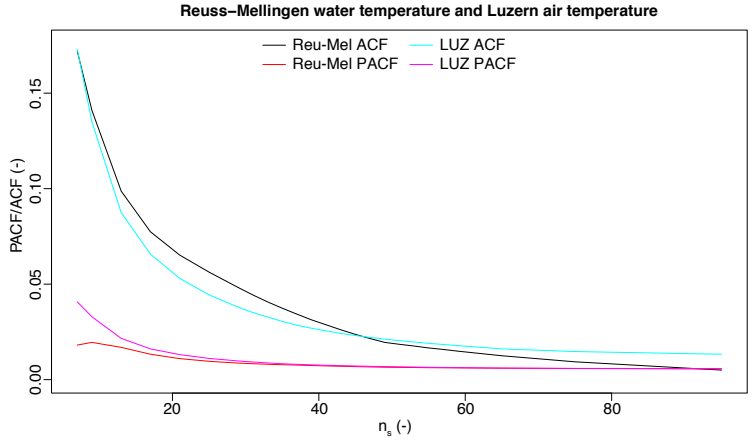

Figure S7. Evolution of the ACF and PACF of the residuals time series of the STL analysis for varying values of n_s for the Reuss water temperature at the FOEN measurement station of Mellingen and for air temperature at the MeteoSwiss measurement station of Luzern.

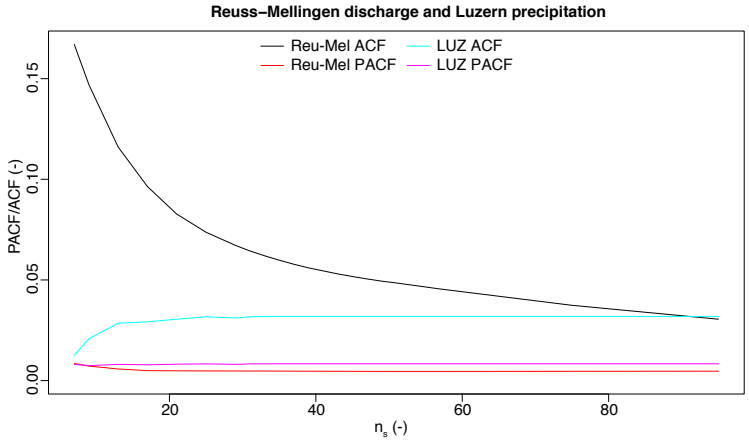

Figure S8. Evolution of the ACF and PACF of the residuals time series of the STL analysis for varying values of n_s for the Reuss discharge at the FOEN measurement station of Mellingen and for precipitation at the MeteoSwiss measurement station of Luzern.

S1.4 Linear trend robustness analysis details

This section shows the analysis of the trend robustness done by comparing the simple linear model with a robust linear model (Figures S9 and S10) and by removing one year at the beginning or at the end of the period (Figures S11 and S12). This robust linear model method (Hampel, 1986) is implemented in the *rlm* function from the MASS package in R (see https://www.rdocumentation.org/packages/MASS/versions/7.3-51.4/topics/rlm for details).

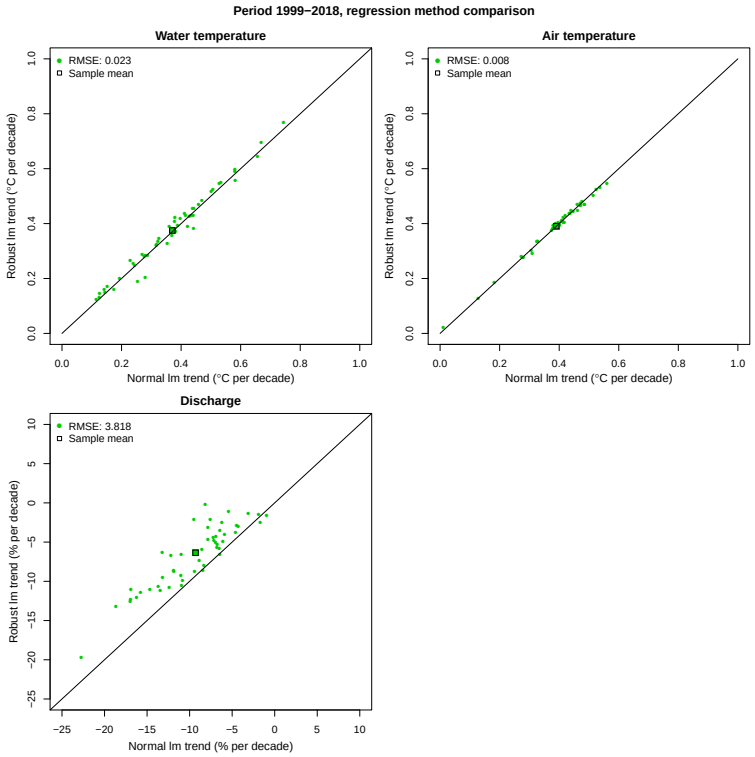

Figure S9. Robust trends plotted against simple linear regression trends for the period 1999-2018 for water temperature (top-left), air temperature (top-right), and discharge (bottom-left). The square indicates the mean value and the RMSE is indicated in °C (top) or in % (bottom).

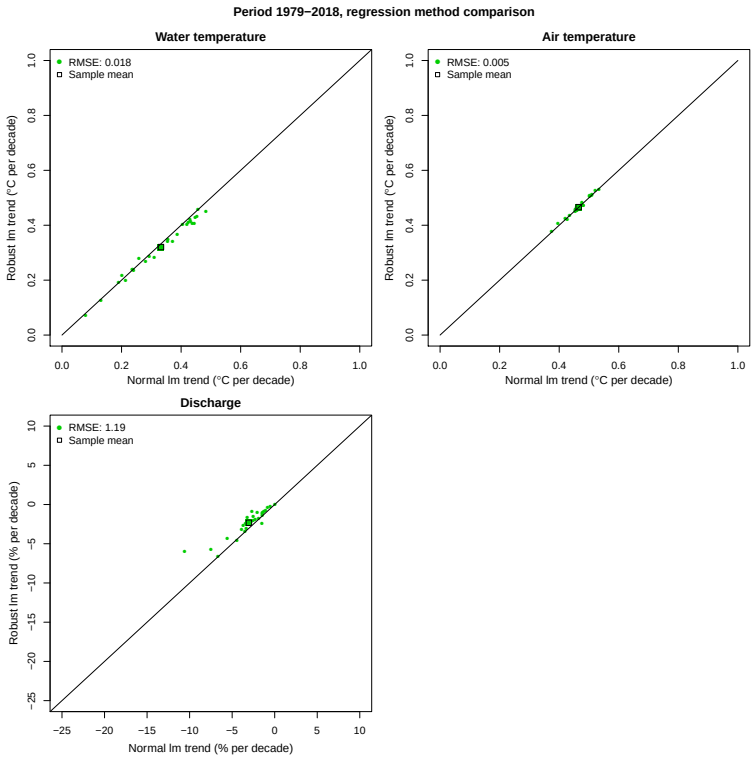

Figure S10. Robust trends plotted against simple linear regression trends for the period 1979-2018 for water temperature (top-left), air temperature (top-right), and discharge (bottom-left). The square indicates the mean value and the RMSE is indicated in °C (top) or in % (bottom).

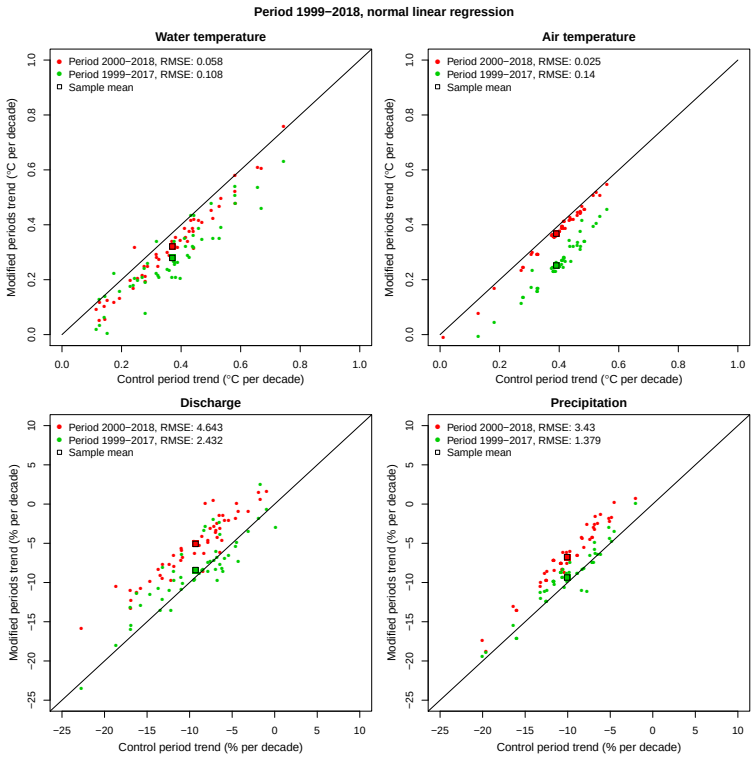

Figure S11. Trends for the period 2000-2018 (red) and 1999-2017 (green) plotted against trends for the period 1999-2018 for water temperature (top-left), air temperature (top-right), discharge (bottom-left) and precipitation (bottom-right). The square indicates the mean value and the RMSE is indicated in °C (top) or in % (bottom).

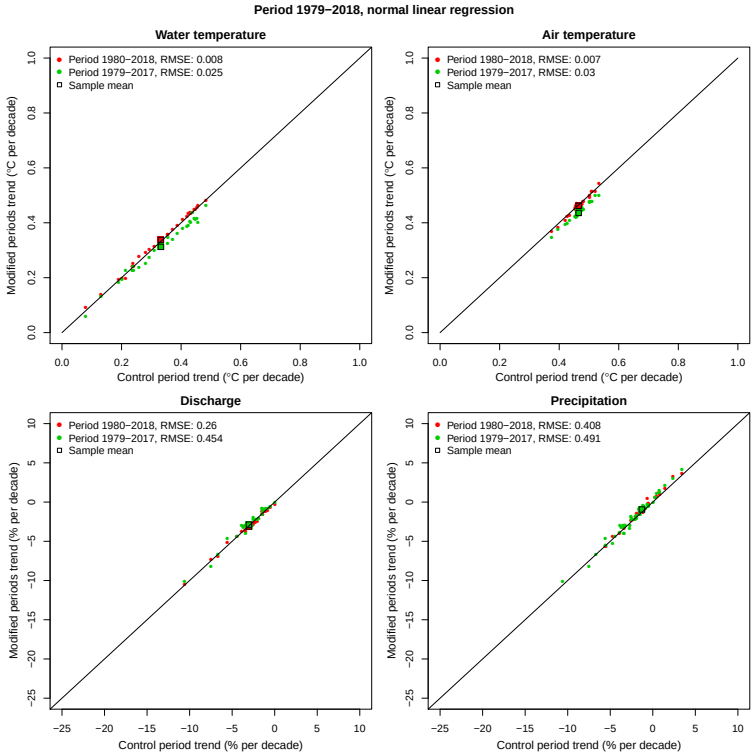

Figure S12. Trends for the period 1980-2018 (red) and 1979-2017 (green) plotted against trends for the period 1979-2018 for water temperature (top-left), air temperature (top-right), discharge (bottom-left) and precipitation (bottom-right). The square indicates the mean value and the RMSE is indicated in °C (top) or in % (bottom).

S2 Supplementary material about results

S2.1 Long-term and trend analysis

This Section presents additional results for Sections 4.1 and 4.2 of the main article. Figure S13 shows the decadal mean of air temperature anomaly (similar to Figure 2b and Figure 4 in the main text), Table S3 presents the results of the two-sided Wilcoxon test used to assess whether differences between regimes are significant in terms of temperature trends, and Figure S14 shows the air temperature and precipitation trends for the four different regimes, and classified upon area, elevation, and glacier-covered fraction, as Figure 6 in the main text.

Figure S15 shows the evolution of the climatic indices used in Lehre Seip et al. (2019). These indices are the North Atlantic Oscillation (NAO) (Jones et al., 1997), and the Atlantic Multi-decadal Oscillation (AMO) (Enfield et al., 2001). Data are obtained from the NOAA website. Long-term decadal anomalies in precipitation and discharge are shown in the figure for comparison purposes.

Tables S4 and S5 show the trends for air temperature and precipitation for the MeteoSwiss station used (see Table S2), for the periods 1999-2018 and 1979-2018. They are similar to Tables A1 and A2 for water temperature and discharge in the Appendix of the main text. Figures S16, S17, and S18 show the same as Figures 5 and 6 in the main text and as Figure S14, but for the period 1979-2018.

Finally, Figure S19 shows the distribution of area for the four different regimes and the distribution of the SPJ water temperature trends as function of the catchment area, showing that there is no correlation between the observed water temperature trend and the catchment area (only SPJ catchments are plotted to separate the effect of regime and the effect of area). Figures S20 and S21 show water temperature trends for each catchment plotted against trends in air temperature for periods 1999-2018 and 1979-2018. While the mean trend values and the distributions are quite similar, single values (i.e. water and air temperature trends for a given catchment) are poorly correlated. Plot over the longest time period show a better correlation for DLA and SPJ catchments, suggesting that part of the poor correlation in Figure S20 is due to the noise in the linear model method. For ALP and HYP catchments, the poor correlation even on longer period suggests a higher influence of other factors than air temperature.

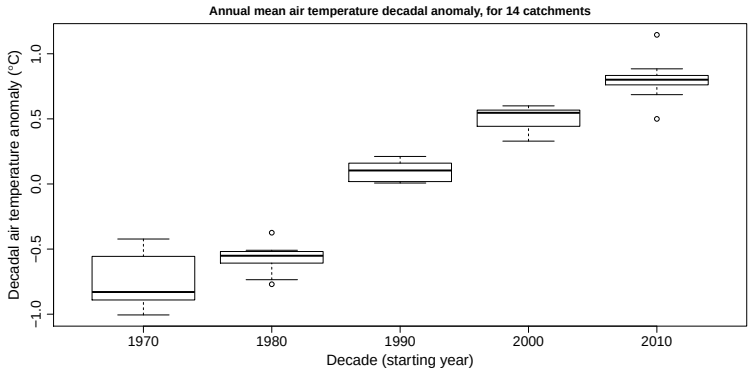

Figure S13. Air temperature anomalies per decade with respect to the 1970-2018 mean, for the 14 catchments with data available since 1970 (same catchments as for water temperature in Figure 2b in main text).

Table S3. P-values of Wilcoxon two-sided test between the trends in water temperature for the four hydrological regimes, period 1999-2018 (left) and 1979-2018 (right).

Period 1999-2018 52 catchments				**Period 1979-2018 28 catchments**			
	ALP	**SPJ**	**HYP**		**ALP**	**SPJ**	**HYP**
DLA	0.008	0.672	0.031	**DLA**	0.005	0.18	6.3e-6
ALP	-	0.019	0.519	**ALP**	-	0.024	0.833
SPJ	-	-	0.046	**SPJ**	-	-	0.002

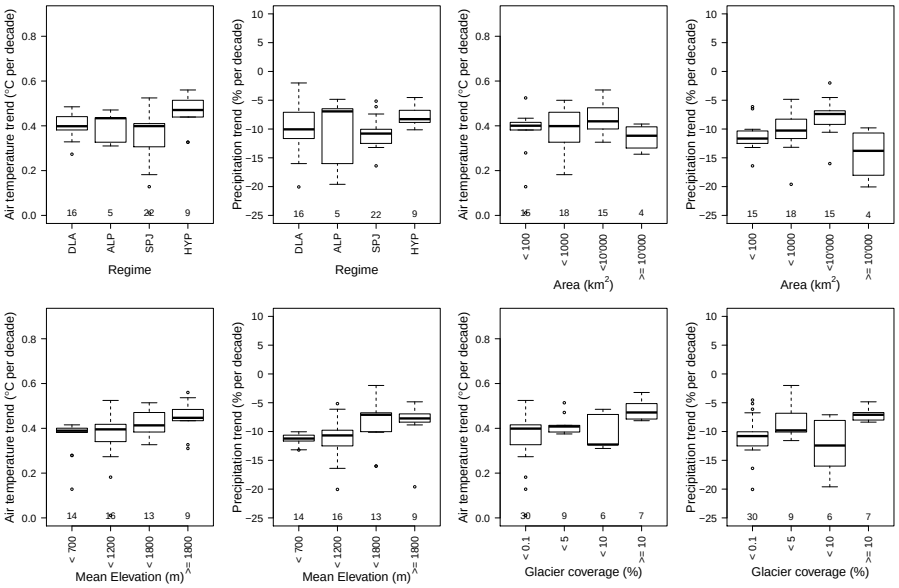

Figure S14. Air temperature and precipitation trends for the 1999–2018 period classified by the four different hydrological regimes – downstream lake regime (DLA), alpine regime (ALP), Swiss Plateau/Jura regime (SPJ), and strong influence from hydro-peaking (HYP) (top-left two panels); by the catchment area (top-right two panels); by the catchment mean elevation (bottom-left two panels); and by the glacier coverage (bottom-right two panels). The numbers along the bottom of the panels indicate the number of catchments in each category.

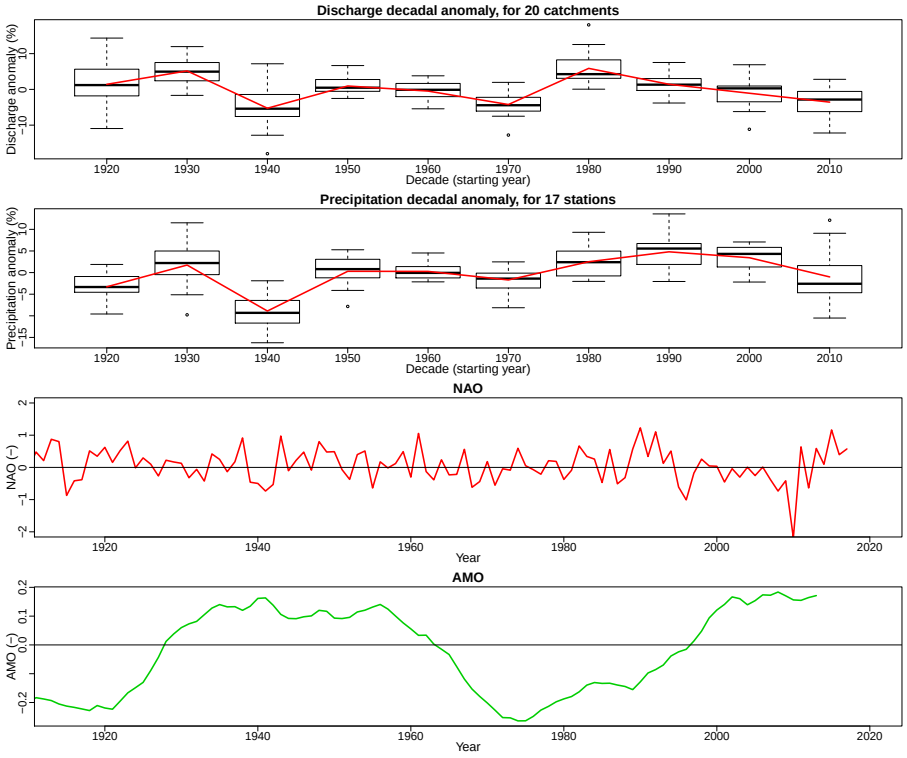

Figure S15. Relative discharge and precipitation decadal means of anomalies with respect to the 1920-2018 average for 20 catchments and 22 MeteoSwiss homogeneous stations with data available since 1920 (upper two plots). Yearly mean of the NAO and AMO (lower two plots).

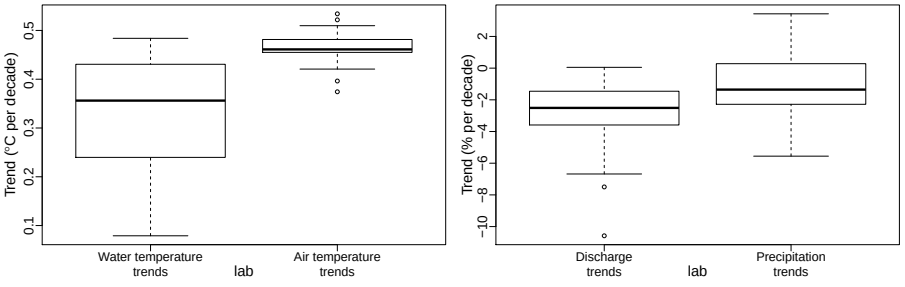

Figure S16. Distributions of trends of water and air temperature (left) , and normalized discharge and normalized precipitation (right), for the periods 1979-2018 for the 27 catchments where data are available for temperature and discharge (see Table 1 in main text).

Table S4. Air temperature (left part) and precipitation (right part) annual and seasonal trends for all the MeteoSwiss stations presented in Table S2 over the period 1999-2018. The numbers in brackets indicate the standard error of the computed trends based on linear regression.

	Water temperature trend (°C per decade)					Discharge trend (% per decade)				
River name	**Annual**	**Winter**	**Spring**	**Summer**	**Autumn**	**Annual**	**Winter**	**Spring**	**Summer**	**Autumn**
ABO	0.44 (0.11)	0.32 (0.12)	0.15 (0.17)	0.56 (0.12)	0.61 (0.13)	-6.9 (4)	-3.1 (15.2)	-7.4 (5.7)	-11.7 (4.6)	-10.8 (5.2)
ALT	0.33 (0.17)	0.20 (0.12)	0.13 (0.17)	0.49 (0.16)	0.43 (0.18)	-8.9 (2.4)	-6.4 (12.1)	-13.3 (4.6)	-6.2 (4.5)	-16.6 (4.8)
BAS	0.35 (0.15)	0.09 (0.08)	0.14 (0.15)	0.70 (0.19)	0.35 (0.07)	-8.5 (4.5)	18.2 (4.5)	-8.5 (3.5)	-10.5 (5.7)	-28.6 (4)
BEH	0.13 (0.13)	0.26 (0.17)	-0.23 (0.17)	0.01 (0.20)	0.40 (0.18)	-37.7 (1.5)	-39.9 (13.2)	-55.1 (4.4)	-9.7 (4.3)	-43.1 (4.5)
BER	0.42 (0.14)	0.22 (0.15)	0.17 (0.10)	0.75 (0.13)	0.44 (0.09)	-12.5 (3)	13.4 (9)	-16.3 (6)	-17.1 (1)	-25.5 (5.6)
CDF	0.51 (0.12)	0.35 (0.06)	0.41 (0.15)	0.69 (0.12)	0.50 (0.10)	-9.2 (3.5)	5.1 (9)	-10.1 (5.7)	-8.8 (2.4)	-28.8 (7.1)
CHA	0.53 (0.12)	0.25 (0.26)	0.43 (0.17)	0.60 (0.16)	0.66 (0.20)	-3.1 (6.1)	-21.3 (10.7)	-5.7 (9.3)	14.4 (3)	-6.0 (8)
CHU	0.50 (0.17)	0.43 (0.06)	0.20 (0.19)	0.73 (0.22)	0.58 (0.24)	-12.0 (6.1)	-9.0 (18)	-11.4 (4.9)	-15.3 (8.2)	-20.3 (3.9)
DEM	0.01 (0.13)	-0.07 (0.16)	-0.23 (0.11)	0.27 (0.14)	0.00 (0.07)	-16.4 (3.6)	0.0 (4.7)	-18.4 (3)	-12.4 (1.8)	-36.2 (4)
EIN	0.49 (0.15)	0.32 (0.05)	0.28 (0.17)	0.71 (0.14)	0.52 (0.11)	-16.0 (3.5)	-21.6 (8.9)	-21.2 (5.6)	-11.6 (3.4)	-18.1 (4.2)
ELM	0.52 (0.15)	0.46 (0.07)	0.36 (0.18)	0.61 (0.16)	0.59 (0.18)	-10.8 (4.5)	-13.5 (11.6)	-11.8 (4)	-10.3 (5.4)	-16.3 (3.3)
ENG	0.51 (0.12)	0.41 (0.06)	0.28 (0.15)	0.63 (0.12)	0.61 (0.12)	-5.1 (2.9)	-6.4 (11.6)	-7.4 (6.3)	-3.6 (6.3)	-9.9 (2.5)
GLA	0.43 (0.18)	0.30 (0.05)	0.29 (0.17)	0.58 (0.22)	0.42 (0.17)	-9.5 (3.6)	-7.4 (11)	-15.8 (4.7)	-8.1 (7)	-15.0 (4.5)
GRC	0.50 (0.08)	0.33 (0.22)	0.27 (0.02)	0.67 (0.14)	0.63 (0.18)	-14.1 (5.5)	8.0 (20.4)	-10.6 (4.4)	-17.7 (5.7)	-37.2 (9.7)
GRH	0.43 (0.07)	0.50 (0.24)	0.25 (0.10)	0.41 (0.09)	0.52 (0.17)	-6.0 (4.2)	-12.1 (11.7)	5.6 (4.7)	-7.7 (6.4)	-13.1 (3.5)
GSB	0.45 (0.05)	0.22 (0.18)	0.21 (0.01)	0.59 (0.10)	0.65 (0.09)	-10.5 (4.5)	2.1 (13.4)	-8.8 (1.8)	-22.7 (3.1)	-18.2 (4.4)
GVE	0.33 (0.16)	0.17 (0.14)	0.14 (0.08)	0.54 (0.16)	0.41 (0.14)	-16.0 (2.7)	11.1 (7.4)	-16.6 (2.9)	-21.1 (0.5)	-35.3 (3)
HLL	0.13 (0.16)	0.07 (0.19)	-0.19 (0.14)	0.37 (0.22)	0.19 (0.09)	-25.4 (3.9)	-20.0 (8.6)	-30.4 (2.9)	-17.3 (7.8)	-35.6 (4.7)
INT	0.51 (0.12)	0.39 (0.11)	0.35 (0.08)	0.71 (0.12)	0.52 (0.10)	-3.6 (2.2)	1.9 (13.4)	-3.8 (5)	-5.5 (5.5)	-11.9 (5.1)
KLO	0.41 (0.16)	0.17 (0.14)	0.14 (0.16)	0.73 (0.20)	0.49 (0.06)	-14.7 (2.1)	-2.7 (6.9)	-18.5 (2.6)	-15.7 (4.6)	-24.6 (3.5)
KOP	0.13 (0.13)	0.05 (0.23)	-0.16 (0.10)	0.43 (0.14)	0.12 (0.08)	-13.2 (2.8)	1.3 (7.4)	-9.7 (2.2)	-15.8 (3.4)	-28.1 (6.6)
LAG	0.25 (0.14)	0.00 (0.08)	0.07 (0.10)	0.65 (0.13)	0.18 (0.12)	-11.2 (3.5)	1.1 (6.1)	-9.1 (8.8)	-15.3 (5.3)	-18.4 (4.1)
LUZ	0.39 (0.16)	0.23 (0.14)	0.17 (0.11)	0.63 (0.21)	0.45 (0.11)	-2.0 (2.7)	19.9 (7.6)	-0.4 (7.7)	-9.9 (5.1)	-7.4 (2.2)
MER	0.46 (0.18)	0.38 (0.12)	0.34 (0.12)	0.57 (0.16)	0.45 (0.18)	-10.5 (3.7)	-11.7 (15.1)	-15.1 (5.1)	-7.5 (4.1)	-14.4 (3.5)
MUB	0.40 (0.14)	0.10 (0.17)	0.19 (0.10)	0.77 (0.14)	0.49 (0.08)	-7.6 (3.5)	13.3 (7.6)	-10.8 (4.3)	-10.9 (1.1)	-18.3 (7.9)
NAP	0.53 (0.11)	0.35 (0.22)	0.34 (0.18)	0.64 (0.16)	0.64 (0.18)	-8.3 (4.1)	2.8 (11.4)	-11.5 (6.9)	-11.5 (6)	-12.6 (5.9)
NEU	0.38 (0.12)	0.13 (0.10)	0.18 (0.08)	0.63 (0.16)	0.50 (0.07)	-9.9 (2.4)	8.0 (7.5)	-3.7 (1.2)	-15.6 (0.2)	-30.1 (5.3)
OTL	0.47 (0.07)	0.40 (0.14)	0.24 (0.06)	0.61 (0.16)	0.61 (0.17)	-9.1 (3)	22.2 (3.7)	-1.4 (1.1)	-17.9 (6.1)	-20.1 (6.4)
PAY	0.31 (0.14)	0.13 (0.13)	0.05 (0.10)	0.54 (0.13)	0.43 (0.08)	-10.4 (1.8)	16.7 (8.6)	-17.3 (0.7)	-9.5 (3.6)	-26.7 (6.1)
RAG	0.30 (0.18)	0.46 (0.03)	0.04 (0.22)	0.37 (0.19)	0.23 (0.22)	-0.2 (5)	-6.1 (12.7)	5.1 (4.5)	-6.0 (5.3)	-3.9 (4.9)
SAE	0.39 (0.11)	0.24 (0.21)	0.24 (0.23)	0.63 (0.08)	0.41 (0.21)	-7.8 (3.3)	-1.1 (11.5)	-17.1 (5.4)	-7.4 (5.9)	-14.2 (6.1)
SAM	0.38 (0.06)	0.84 (0.13)	-0.01 (0.10)	0.35 (0.07)	0.36 (0.16)	-8.6 (3.6)	24.5 (4.4)	0.0 (1.3)	-7.3 (4.1)	-34.5 (6.3)
SBE	0.48 (0.05)	0.35 (0.19)	0.32 (0.06)	0.52 (0.15)	0.62 (0.12)	0.0 (6.4)	27.6 (1.6)	7.0 (3.9)	-2.9 (6.7)	-16.4 (7.7)
SIA	0.42 (0.05)	0.51 (0.21)	0.19 (0.01)	0.56 (0.09)	0.40 (0.14)	-12.5 (3.1)	6.3 (9.1)	-7.1 (5.7)	-11.9 (4.3)	-28.5 (7.2)
SIO	0.67 (0.16)	0.42 (0.09)	0.37 (0.10)	1.03 (0.18)	0.78 (0.20)	-4.9 (5.8)	23.2 (16.6)	-8.3 (3.8)	-19.1 (1.4)	-21.7 (3.7)
SMA	0.38 (0.15)	0.10 (0.07)	0.15 (0.16)	0.70 (0.20)	0.46 (0.10)	-11.7 (4.6)	-1.1 (7.4)	-21.1 (5.6)	-5.3 (5.5)	-23.2 (3.9)
STG	0.33 (0.13)	0.17 (0.07)	0.14 (0.21)	0.50 (0.15)	0.40 (0.12)	0.3 (3.4)	22.5 (10.3)	-8.8 (9)	-0.4 (2.5)	-7.9 (3.6)
TAE	0.42 (0.15)	0.24 (0.10)	0.11 (0.19)	0.71 (0.16)	0.49 (0.06)	-9.9 (2.2)	-1.3 (7.7)	-17.6 (4.8)	-5.0 (5)	-18.1 (4.9)
VAD	0.52 (0.17)	0.35 (0.03)	0.24 (0.23)	0.79 (0.15)	0.55 (0.16)	-8.0 (4.6)	-9.6 (14.1)	-9.0 (9.9)	-9.6 (3.6)	-10.2 (3.5)
WAE	0.46 (0.16)	0.32 (0.12)	0.20 (0.13)	0.68 (0.21)	0.54 (0.11)	-9.5 (4.5)	-0.7 (9.4)	-15.8 (7.3)	-7.0 (5.5)	-20.8 (4.6)
WYN	0.43 (0.16)	0.28 (0.15)	0.20 (0.12)	0.69 (0.17)	0.47 (0.08)	-8.1 (1.9)	4.5 (8.9)	-5.4 (1)	-8.9 (4.7)	-23.8 (7.7)

Table S5. Air temperature (left part) and precipitation (right part) annual and seasonal trends for all the MeteoSwiss stations presented in Table S2 over the period 1979-2018. The numbers in brackets indicate the standard error of the computed trends based on linear regression.

	Water temperature trend (°C per decade)					Discharge trend (% per decade)				
River name	**Annual**	**Winter**	**Spring**	**Summer**	**Autumn**	**Annual**	**Winter**	**Spring**	**Summer**	**Autumn**
BER	0.48 (0.03)	0.28 (0.01)	0.61 (0.02)	0.65 (0.03)	0.34 (0.03)	-3.9 (0.5)	-2.4 (2.6)	-3.5 (0.3)	-2.6 (0.7)	-8.8 (1.7)
INT	0.52 (0.02)	0.26 (0.02)	0.70 (0.01)	0.69 (0.03)	0.40 (0.03)	0.1 (0.6)	-3.7 (3.1)	1.0 (1.3)	3.1 (0.7)	-3.8 (1.8)
GRH	0.43 (0.02)	0.22 (0.05)	0.68 (0.02)	0.58 (0.02)	0.20 (0.05)	-2.8 (0.2)	-6.6 (1.7)	-1.6 (0.9)	-1.3 (1.7)	-0.7 (1.2)
MER	0.50 (0.04)	0.36 (0.03)	0.67 (0.02)	0.57 (0.04)	0.33 (0.05)	-1.2 (0.3)	-9.1 (2.1)	-1.7 (0.9)	3.5 (0.9)	-2.3 (1)
SMA	0.46 (0.03)	0.29 (0.01)	0.61 (0.02)	0.60 (0.05)	0.31 (0.03)	-0.9 (0.7)	-4.0 (1.8)	1.8 (1.5)	1.6 (1.6)	-6.5 (1.4)
WYN	0.44 (0.03)	0.29 (0.02)	0.55 (0.01)	0.60 (0.04)	0.30 (0.03)	-1.2 (0.3)	-5.2 (2.3)	1.6 (0.4)	2.6 (1.5)	-6.7 (2.2)
PAY	0.44 (0.03)	0.26 (0.02)	0.55 (0.02)	0.59 (0.03)	0.30 (0.03)	-3.9 (0.1)	-7.0 (3.3)	-3.1 (0.5)	-2.3 (1.8)	-6.1 (2)
NEU	0.41 (0.02)	0.24 (0.01)	0.57 (0.02)	0.50 (0.04)	0.29 (0.03)	-2.3 (0.1)	-3.8 (2.2)	-0.7 (0.2)	2.1 (1.3)	-9.7 (1.8)
GVE	0.46 (0.03)	0.21 (0.02)	0.62 (0.00)	0.60 (0.03)	0.34 (0.04)	-5.6 (0.1)	-9.5 (3.1)	-4.7 (0.4)	-1.3 (1.4)	-8.5 (1.8)
BAS	0.49 (0.03)	0.34 (0.03)	0.59 (0.02)	0.66 (0.04)	0.35 (0.02)	1.1 (0.8)	0.1 (1.7)	1.8 (0.7)	1.7 (1.8)	-0.8 (1.9)
DEM	0.43 (0.02)	0.32 (0.02)	0.54 (0.01)	0.54 (0.02)	0.26 (0.01)	-4.4 (0.5)	-6.2 (1.3)	-7.4 (0.9)	-0.2 (0.6)	-6.1 (1.9)
LAG	0.31 (0.03)	0.23 (0.01)	0.45 (0.01)	0.32 (0.04)	0.19 (0.03)	-6.8 (0.5)	-12.2 (1.7)	-4.9 (0.4)	-3.5 (1.5)	-10.2 (1)
NAP	0.44 (0.03)	0.12 (0.05)	0.72 (0.03)	0.63 (0.04)	0.24 (0.06)	4.5 (1)	4.6 (1.9)	7.5 (1.6)	4.7 (2)	-0.3 (1.8)
ENG	0.43 (0.03)	0.21 (0.01)	0.61 (0.02)	0.56 (0.03)	0.30 (0.04)	0.1 (0.5)	-4.4 (2.5)	2.2 (0.9)	2.4 (1.7)	-3.4 (1.1)
KLO	0.45 (0.03)	0.34 (0.03)	0.56 (0.02)	0.57 (0.05)	0.28 (0.02)	1.8 (0.6)	-0.9 (1.6)	4.4 (1.4)	3.5 (1.8)	-3.3 (1.5)
SAM	0.52 (0.01)	0.59 (0.03)	0.60 (0.00)	0.51 (0.01)	0.39 (0.04)	-2.6 (1)	-0.8 (1.7)	-6.9 (0.7)	-1.3 (1.2)	-3.7 (2.5)
SIA	0.45 (0.01)	0.40 (0.05)	0.64 (0.02)	0.42 (0.02)	0.33 (0.04)	-2.9 (1.3)	-2.4 (2.3)	-10.2 (1.6)	-1.2 (1.3)	-0.5 (2.5)
BEH	0.26 (0.04)	0.28 (0.05)	0.48 (0.06)	0.18 (0.05)	0.11 (0.05)	-8.6 (0.9)	-4.1 (1.4)	-20.8 (1.2)	-3.0 (1.3)	-5.5 (1)
LUZ	0.48 (0.03)	0.28 (0.01)	0.63 (0.01)	0.62 (0.05)	0.33 (0.03)	2.4 (0.9)	-1.1 (2.5)	4.8 (0.8)	4.4 (1.7)	-2.4 (1.4)
WAE	0.46 (0.04)	0.41 (0.00)	0.58 (0.02)	0.53 (0.06)	0.33 (0.04)	-2.3 (0.8)	-6.1 (2.1)	-2.1 (2.1)	1.0 (1.6)	-6.3 (1.5)
GLA	0.44 (0.04)	0.27 (0.03)	0.61 (0.03)	0.57 (0.05)	0.27 (0.05)	-0.6 (0.8)	-4.4 (1.8)	-1.2 (1.5)	1.0 (2)	-1.4 (1.5)
ELM	0.48 (0.03)	0.30 (0.02)	0.70 (0.03)	0.56 (0.04)	0.31 (0.05)	-2.3 (0.4)	-4.9 (2.5)	-2.9 (1.2)	-0.4 (1.6)	-3.6 (1.2)
RAG	0.45 (0.04)	0.35 (0.03)	0.58 (0.03)	0.53 (0.04)	0.29 (0.05)	-1.4 (1.3)	-4.7 (2.4)	0.1 (2.9)	-2.6 (1.4)	-0.5 (2.2)
ABO	0.36 (0.03)	0.14 (0.03)	0.60 (0.02)	0.46 (0.03)	0.22 (0.05)	-3.9 (0.8)	-9.5 (3.5)	-1.8 (1.2)	-0.9 (1.4)	-7.9 (1.6)
ALT	0.48 (0.03)	0.28 (0.02)	0.64 (0.02)	0.61 (0.03)	0.35 (0.05)	0.3 (0.3)	-4.5 (2.6)	-0.2 (0.8)	3.1 (1.4)	-1.9 (1.4)
VAD	0.56 (0.04)	0.43 (0.02)	0.69 (0.04)	0.69 (0.04)	0.37 (0.05)	0.3 (0.5)	-5.4 (3.1)	4.0 (1.1)	0.5 (1.2)	-1.9 (1)
CHU	0.59 (0.04)	0.40 (0.04)	0.72 (0.03)	0.76 (0.05)	0.45 (0.06)	-0.9 (1.4)	-4.1 (4.1)	-2.9 (2.5)	0.9 (2.5)	-1.8 (2)
HLL	0.41 (0.03)	0.38 (0.02)	0.48 (0.01)	0.44 (0.05)	0.30 (0.02)	-6.9 (0.7)	-10.3 (1.6)	-5.8 (1.1)	-0.2 (2)	-13.1 (1.4)
SIO	0.63 (0.04)	0.33 (0.01)	0.74 (0.01)	0.80 (0.05)	0.61 (0.05)	-4.2 (0.6)	-4.9 (4.4)	-1.8 (0.8)	2.8 (1)	-16.7 (0.9)
GSB	0.41 (0.02)	0.17 (0.05)	0.66 (0.02)	0.57 (0.02)	0.22 (0.04)	-2.5 (0.7)	-0.5 (3.2)	-4.5 (0.9)	-0.9 (1.5)	-4.9 (0.5)
GRC	0.45 (0.02)	0.12 (0.05)	0.75 (0.02)	0.60 (0.03)	0.30 (0.06)	-7.1 (1.1)	-10.8 (4.8)	-10.1 (0.3)	1.9 (2)	-12.1 (1)
SAE	0.35 (0.03)	0.08 (0.06)	0.62 (0.04)	0.54 (0.04)	0.13 (0.06)	-1.0 (0.4)	1.4 (2.7)	-3.1 (1.4)	0.8 (1.7)	-5.1 (1.7)
STG	0.47 (0.02)	0.29 (0.02)	0.66 (0.03)	0.61 (0.03)	0.28 (0.04)	1.6 (0.4)	3.1 (3.2)	0.7 (1.3)	2.5 (0.6)	-0.7 (1.1)
SBE	0.39 (0.02)	0.20 (0.05)	0.66 (0.02)	0.48 (0.04)	0.22 (0.04)	-0.5 (0.7)	2.4 (1.3)	-6.9 (0.8)	2.3 (0.8)	0.2 (1.4)
OTL	0.52 (0.01)	0.30 (0.03)	0.72 (0.03)	0.61 (0.04)	0.43 (0.05)	-1.5 (0.7)	6.4 (1.4)	-6.8 (0.7)	-2.8 (1.9)	1.0 (0.2)
CDF	0.49 (0.03)	0.23 (0.02)	0.73 (0.02)	0.63 (0.03)	0.34 (0.03)	-4.6 (0.1)	-5.4 (2.3)	-5.4 (0.4)	-1.2 (0.8)	-8.7 (2.2)
CHA	0.36 (0.04)	0.06 (0.07)	0.66 (0.03)	0.50 (0.05)	0.22 (0.07)	-0.4 (0.1)	-11.5 (1.9)	1.9 (0.5)	11.6 (0.6)	-4.9 (2)
KOP	0.34 (0.02)	0.28 (0.01)	0.44 (0.01)	0.38 (0.03)	0.21 (0.01)	-5.0 (0.6)	-10.1 (2)	-4.2 (0.6)	-1.0 (1.3)	-8.2 (2)
TAE	0.46 (0.03)	0.36 (0.02)	0.56 (0.03)	0.59 (0.04)	0.31 (0.02)	-1.7 (0.8)	-5.0 (1.9)	0.3 (1.7)	2.0 (1.4)	-7.4 (1.4)
EIN	0.43 (0.03)	0.28 (0.00)	0.60 (0.03)	0.54 (0.04)	0.26 (0.04)	-4.9 (0.4)	-8.6 (1.5)	-3.4 (1.1)	-3.1 (1)	-7.7 (1.2)

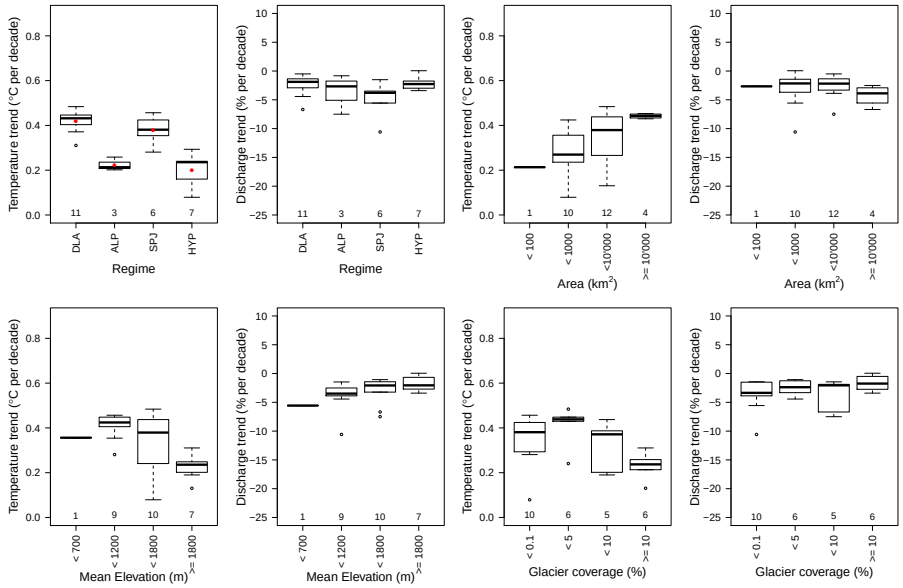

Figure S17. Water temperature and discharge trends for the 1979–2018 period classified by the four different hydrological regimes – downstream lake regime (DLA), alpine regime (ALP), Swiss Plateau/Jura regime (SPJ), and strong influence from hydro-peaking (HYP) (top-left two panels); by the catchment area (top-right two panels); by the catchment mean elevation (bottom-left two panels); and by the glacier coverage (bottom-right two panels). The numbers along the bottom of the panels indicate the number of catchments in each category. In the top-left boxplot, the red dots are the mean values (values used for the Wilcoxon test, see main text and Table S3).

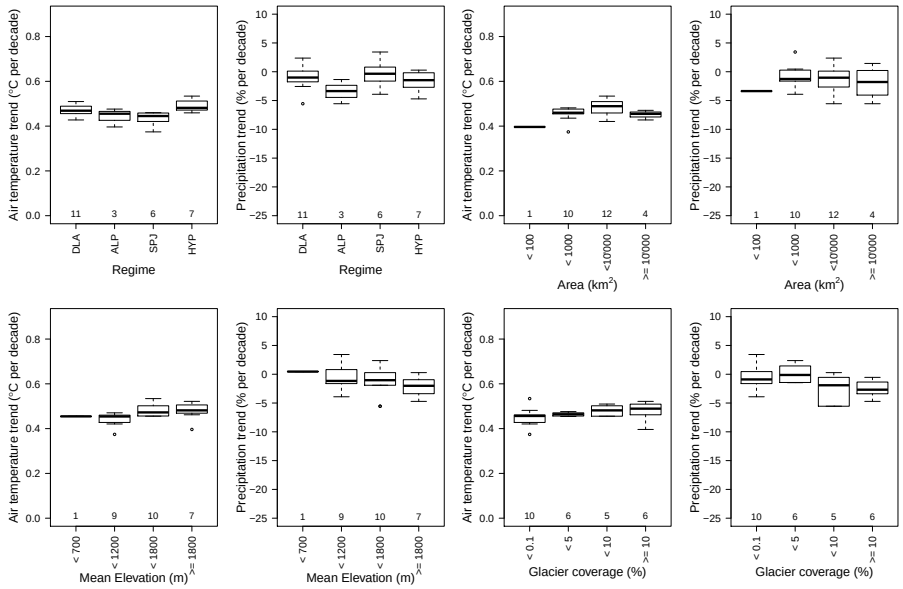

Figure S18. Air temperature and precipitation trends for the 1979–2018 period classified by the four different hydrological regimes – downstream lake regime (DLA), alpine regime (ALP), Swiss Plateau/Jura regime (SPJ), and strong influence from hydro-peaking (HYP) (top-left two panels); by the catchment area (top-right two panels); by the catchment mean elevation (bottom-left two panels); and by the glacier coverage (bottom-right two panels). The numbers along the bottom of the panels indicate the number of catchments in each category.

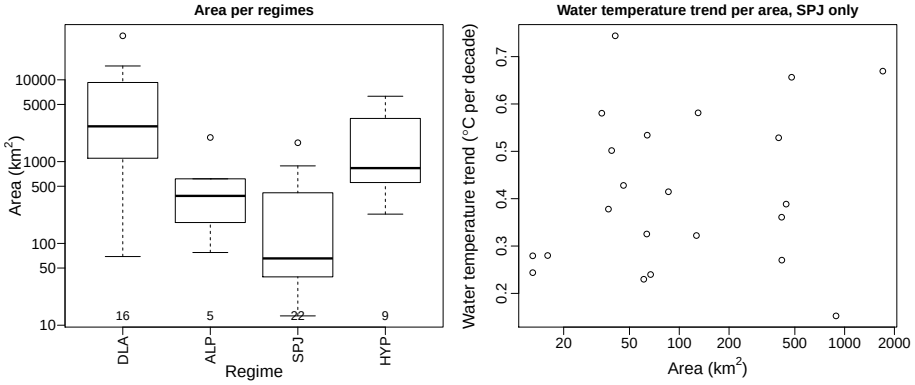

Figure S19. Left: Distribution of catchment area for four different regimes (DLA = downstream lake regimes, ALP = alpine regimes, SPJ = Swiss Pateau/Jura regimes and HYP = strong influence from hydropeaking). Right: Temperature trends for SPJ regime catchments only.

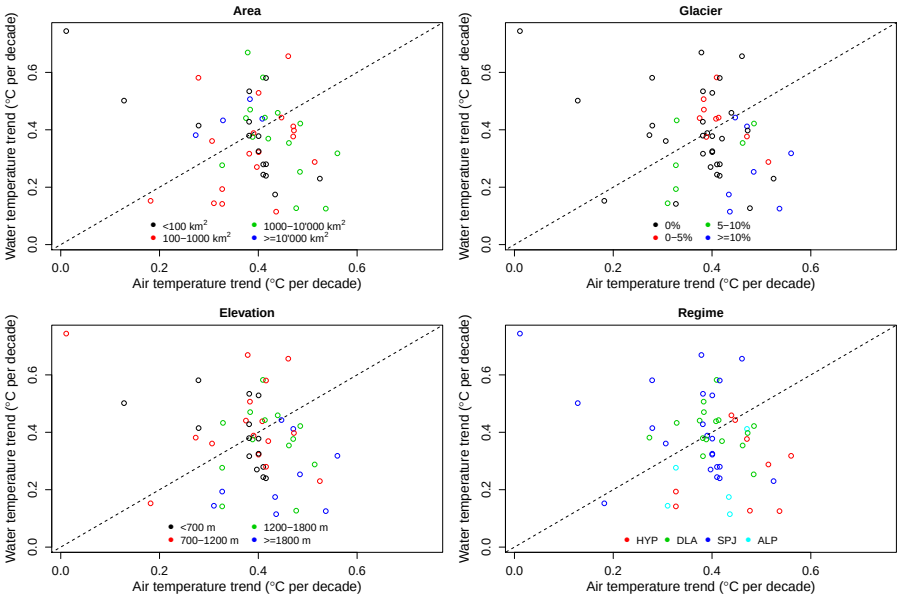

Figure S20. Water temperature trends plotted against air temperature trends. Values are colored by catchment area (top-left), glacier covered catchment fraction (top-right), mean catchment elevation (bottom-left) and regimes (bottom-right). Period 1999-2018.

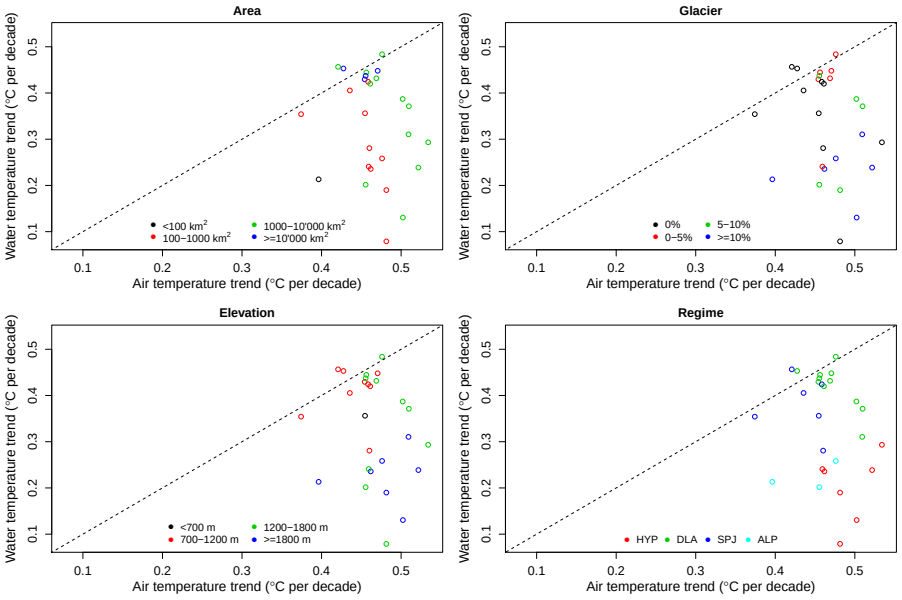

Figure S21. Water temperature trends plotted against air temperature trends. Values are colored by catchment area (top-left), glacier covered catchment fraction (top-right), mean catchment elevation (bottom-left) and regimes (bottom-right). Period 1979-2018.

S2.2 Lake effect

This Section presents plots for the four lakes not shown in the main text Section 4.3: Lake Walen (Figure S22), Lake Luzern (Figure S23), Lakes Brienz and Thun (Figure S24), and Lake Biel (Figure S25). The values for the various trends presented are shown in Table 3 in the main text.

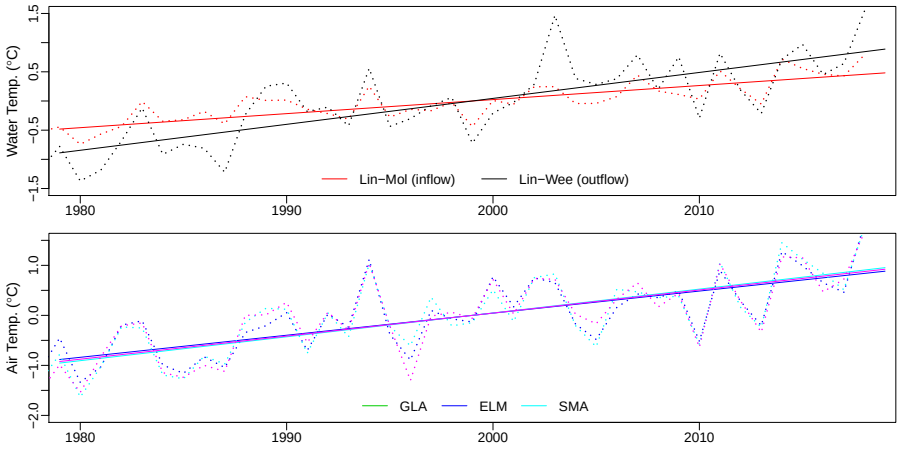

Figure S22. Lake Walen: Water temperature anomalies and trends for inflow and outlet stations (top), air temperature anomalies and trends for surrounding MeteoSwiss stations (bottom). The period for trend computation is 1979-2018. The abbreviation for water gauging stations and for MeteoSwiss stations are given in Table 1 in main text and in Table S2.

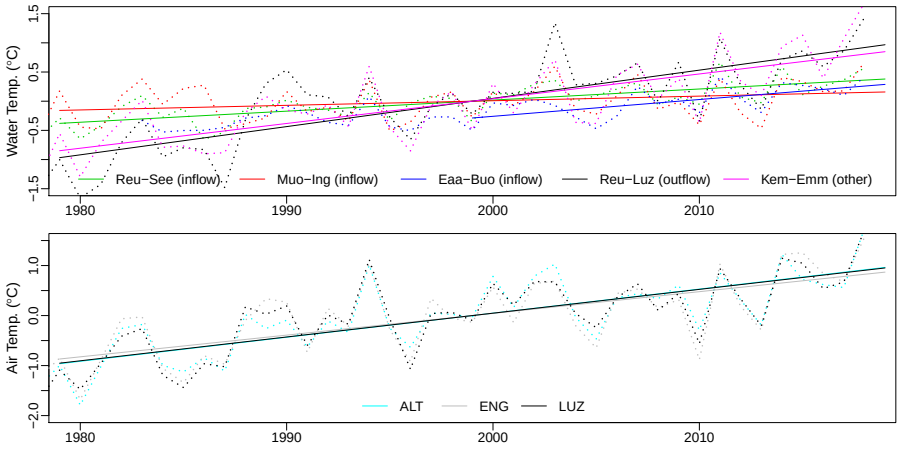

Figure S23. Lake Luzern: Water temperature anomalies and trends for inflow and outlet stations (top), air temperature trends for surrounding MeteoSwiss stations (bottom). The period for trend computation is 1979-2018, except for the Engelberger Aa in Buochs (Eaa-Buo) where the trend is computed over the period 1999-2018. The abbreviation for water gauging stations and for MeteoSwiss stations are given in Table 1 in main text and in Table S2.

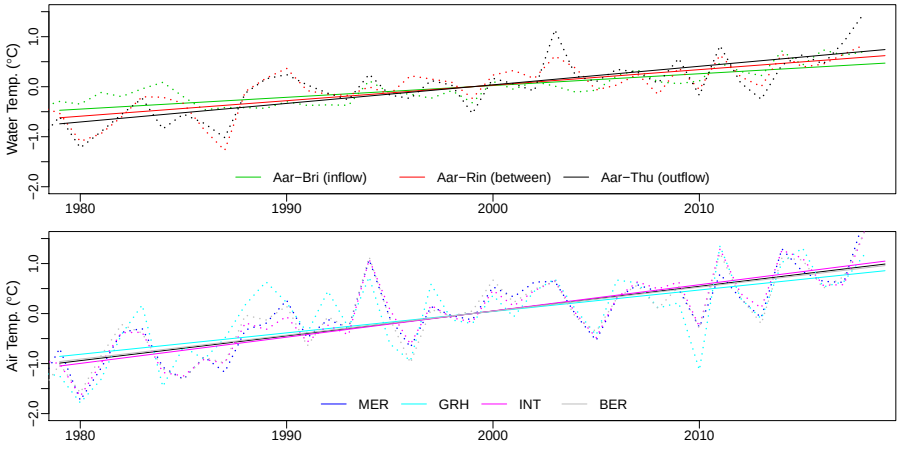

Figure S24. Lakes Brienz and Thun: Water temperature anomalies and trends for inflow and outlet stations (top), air temperature anomalies and trends for surrounding MeteoSwiss stations (bottom). The period for trend computation is 1979-2018. The abbreviation for water gauging stations and for MeteoSwiss stations are given in Table 1 in main text and in Table S2.

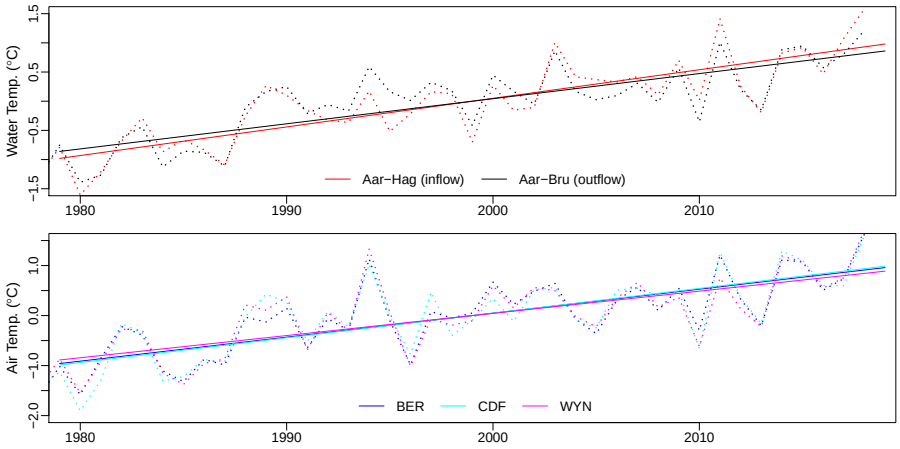

Figure S25. Lake Biel: Water temperature anomalies and trends for inflow and outlet stations (top), air temperature anomalies trends for surrounding MeteoSwiss stations (bottom). The period for trend computation is 1979-2018. The abbreviation for water gauging stations and for MeteoSwiss stations are given in Table 1 in main text and in Table S2.

S2.3 Seasonal trends and relation with air temperature and precipitation

This Section presents additional results related to Section 4 of the main text. Figures S26 and S27 show the decadal evolution of air temperature and precipitation for the four seasons, similar to Figures 8 and 9 in the main text for stream temperature and discharge.

Table S6 shows the correlation between trends of various variables. As discussed in the main text, these correlations are mostly not significant and thus not considered in the study.

Figures S28, S29 and S30 show the yearly anomalies in stream temperature, discharge, air temperature and precipitation in winter and autumn, similar to Figures 11 in the main text which presents summer.

Figure S31 shows the snow water equivalent (SWE) at the beginning of various months over the whole country, Figure S32 the evolution of spring melt, obtained by subtracting first of June to first of March SWE, and Figure S33 shows the evolution of the summer mass balance for 7 Swiss glaciers.

Finally, Figure S34 and Table S7 show additional content for Section 4.4.5 of the main text. Figure S34 shows the annual difference between summer and winter means for all catchments with data since at least 1980. A 5-year moving average window is applied for noise reduction. Note the $\sim$14 years cycle present in the data with an amplitude of about 0.5 °C, probably caused by large scale atmospheric phenomena (as also found in Webb and Nobilis (2007)). The year-to-year variations of the temperature difference anomaly are more driven by this oscillation than by the underlying trend. Nevertheless, there is a clear evolution on the intra-annual variability: the computed trend indicates an increase of 0.3±0.1 °C per decade, which corresponds to a change of +1.2 °C over the studied period. The mean raw intra-annual variability equals 9.8 °C, with a standard deviation of 3.6 °C. This represents an increase of 10% to 20% of the variability for individual catchments.

Table S7 shows the correlations between water temperature and water temperature from previous seasons, between discharge and precipitation from previous seasons, and between water temperature and precipitation from previous. They were obtained with the same method as the data in Table 3 in main text. This Table shows that for water temperature there is almost no correlation and calculated values are mostly not significant. The only observed signal is from one season directly to the next one, but it is far weaker and less significant than the correlation with air temperature during the same season (see Table 3 in main text). There is also no strong correlation between precipitation and discharge more than one season apart. The correlation with the next season is weak and significant only for a few catchments, showing that the groundwater storage plays an important buffer role. A weak correlation is also seen between winter and the following summer, showing the influence of the remaining snow in summer for a few catchments. Regarding correlation between precipitation and water temperature, only two values are significant for more than 10 catchments. There is a negative correlation between spring precipitation and summer stream temperature, which is discussed in the main text. There is also a positive significant correlation for 15 catchments from spring to the following year spring, but since no real physical process was found to explain it, it is assumed to be noise in the results.

Finally, Figure S35 shows some additional details about alpine catchments discussed in Section 4.4.4 in the main text and Figures S36 and S37 show plots similar to Figure 15 in the main text but for the Arve River in Geneva and for the Lütschine River in Gsteig.

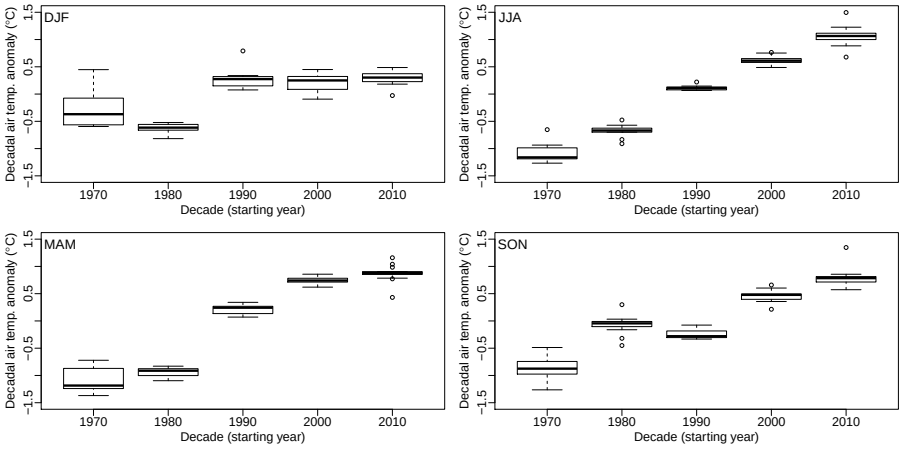

Figure S26. Air temperature seasonal anomalies for the 14 catchments where data are available since 1970 (see Table S2). Anomalies with respect to the 1970-2018 period.

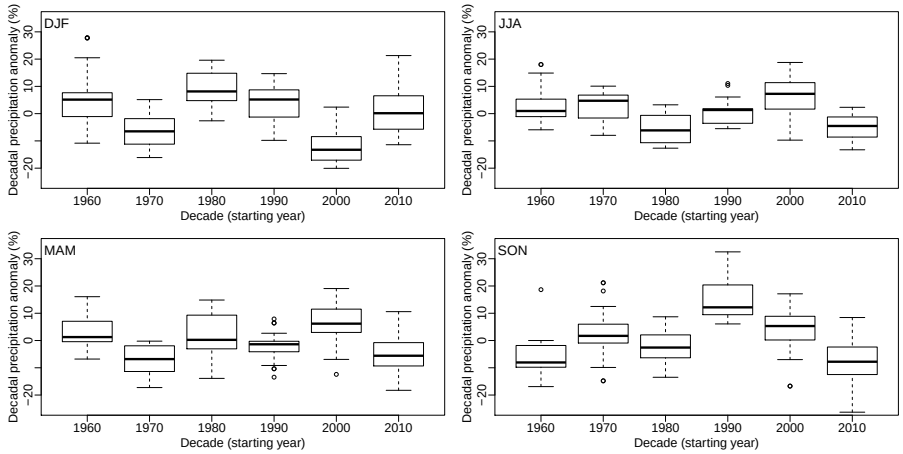

Figure S27. Precipitation seasonal relative anomalies for the 26 stations where data are available since 1960 (see Table S2). Anomalies with respect to 1960-2018 period.

Table S6. Correlation between the trends of water and air temperature (left), water temperature and discharge (middle) and discharge and precipitation (right). Correlations are computed between annual and seasonal trends, and by taking one value per catchment and constructing ordered vectors of values. The number in parenthesis indicates the p-value of the null-hypothesis (no correlation). Since the computation here is different from the one in Table 4 in main text (where correlation is computed from full time series and then averaged between catchment), the two tables cannot be compared.

Water and air temperature trends		**Water temperature and discharge trends**		**Discharge and precipitation trends**	
Period	**cor.**	**Period**	**Cor.**	**Period**	**Cor.**
Yearly	-0.18 (0.19)	Yearly	-0.25 (0.08)	yearly	0.08 (0.01)
Winter	-0.13 (0.36)	Winter	-0.50 (<0.01)	Winter	0.36 (0.02)
Spring	0.02 (0.87)	Spring	-0.35 (0.01)	Spring	0.11 (0.43)
Summer	-0.09 (0.51)	Summer	-0.05 (0.72)	Summer	0.33 (0.01)
Autumn	-0.26 (0.07)	Autumn	-0.26 (0.06)	Autumn	0.34 (0.58)

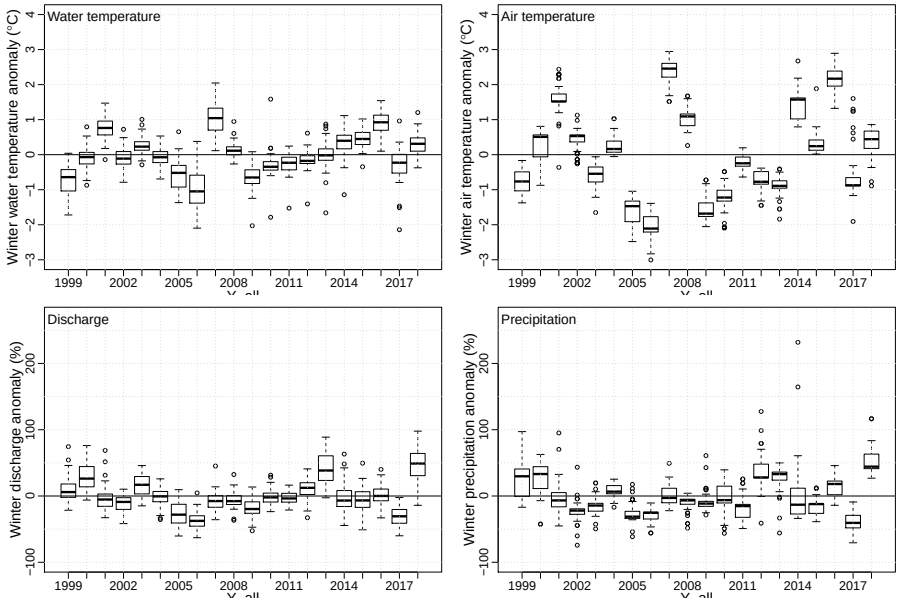

Figure S28. Winter anomalies in stream temperature, air temperature, relative discharge and relative precipitation for all catchments. Anomalies are computed with respect to the 1999-2018 mean for each catchment.

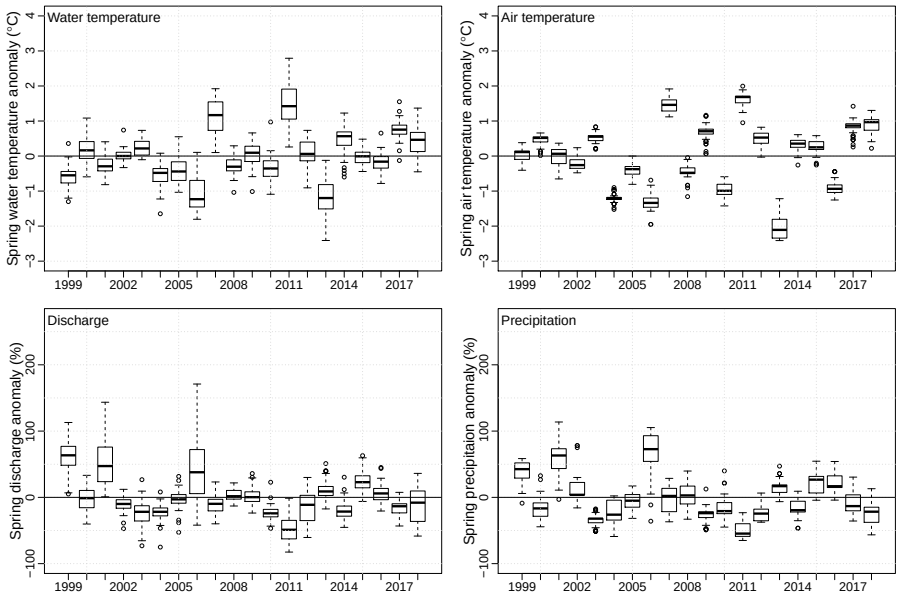

Figure S29. Spring anomalies in water temperature, air temperature, relative discharge and relative precipitation for all 52 catchments. Anomalies are computed with respect to the 1999-2018 mean for each catchment.

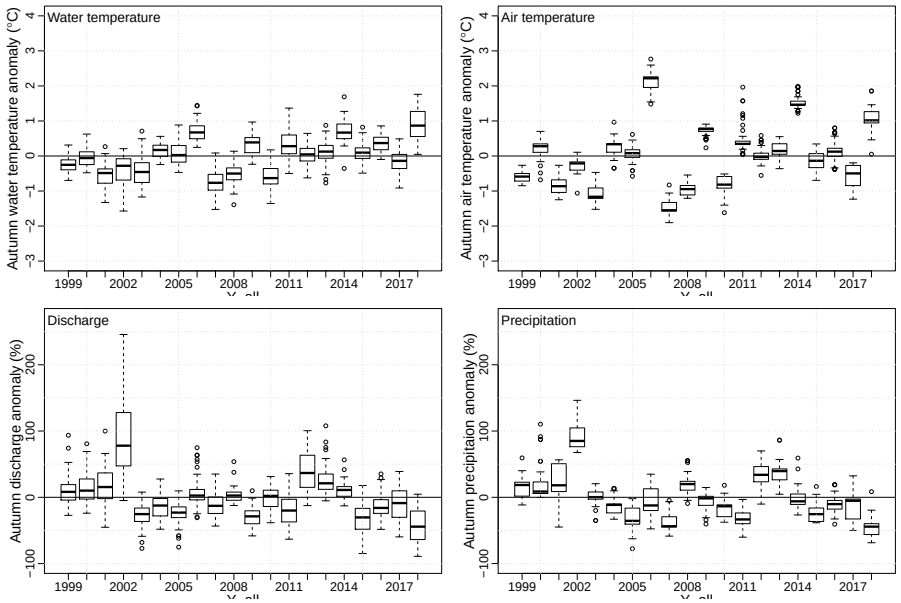

Figure S30. Autumn anomalies in stream temperature, air temperature, relative discharge and relative precipitation for all catchments. Anomalies are computed with respect to the 1999-2018 mean for each catchment.

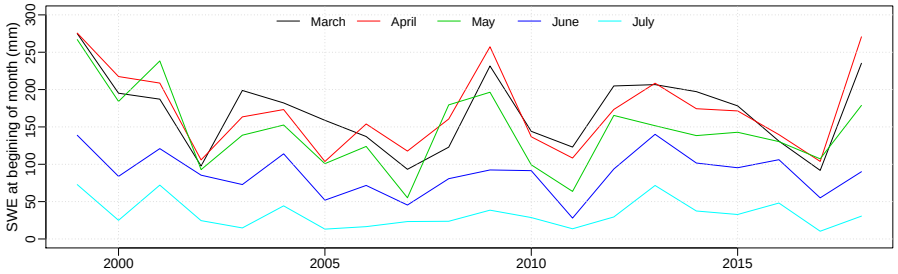

Figure S31. Snow water equivalent in spring over the entire Switzerland at the beginning of the months, from March to July. Obtained from Magnusson et al. (2014) and provided by the WSL Institute for Snow and Avalanche Research (SLF).

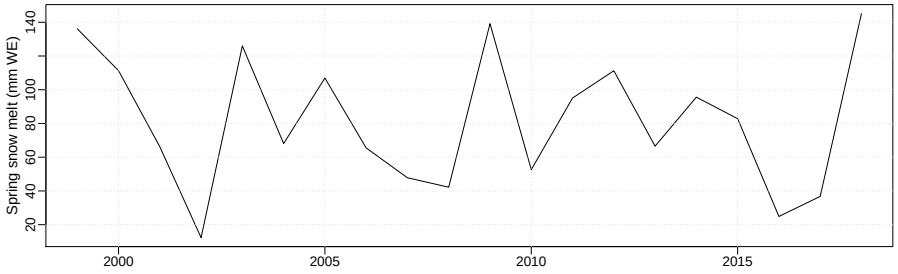

Figure S32. Snow melt evolution in spring over the entire Switzerland, obtained by subtracting first of June to first of March SWE.

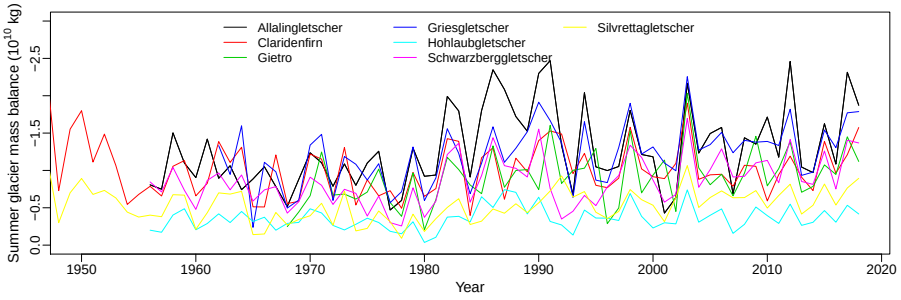

Figure S33. Summer mass balance for 7 Swiss glaciers, from (GLAMOS, 2018).

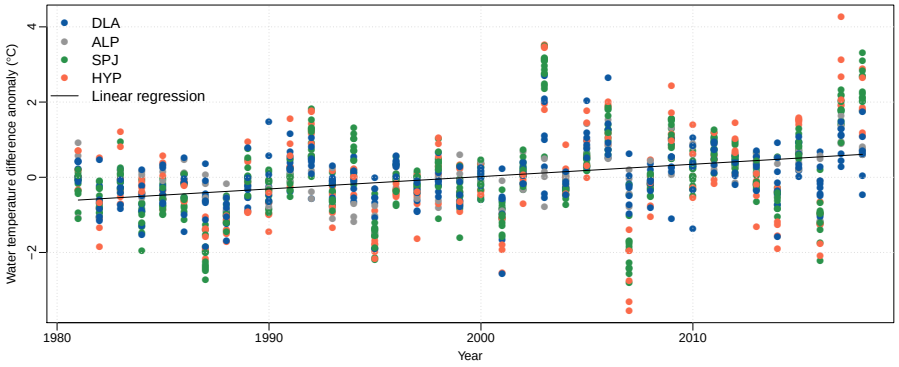

Figure S34. Water temperature summer to winter difference yearly anomalies. The hydrological regimes are represented by the dot colours and the abbreviations are Swiss Plateau and Jura regime (SPJ), Alpine regime (ALP), Downstream lake regime (DLA), and Regime strongly influenced by hydropeaking (HYP). The black line represents the fitted linear regression.

Table S7. Correlation for different seasons between water temperature and itself (left), precipitation and discharge (middle) and precipitation and water temperature (right). The correlations are computed between the season indicated in the line and the next season indicated in the column, (e.g. DJF and MAM shows the correlation between winter and the next spring, while MAM and DFJ shows the correlation between spring and the next winter. Correlation between the same season shows correlation between seasons at one-year lag (i.e. correlation between winters and the next winters). The numbers in brackets indicate the number of catchments where the correlation is not significant (p-value>0.05 for the null hypothesis being no correlation).

	Water temperature to water temperature			
	DJF	**MAM**	**JJA**	**SON**
DJF	0.13 (50)	0.34 (40)	0.02 (50)	-0.09 (52)
MAM	0.13 (52)	-0.18 (48)	0.36 (36)	0.04 (50)
JJA	0.14 (50)	-0.08 (48)	0.10 (48)	0.28 (39)
SON	0.28 (44)	0.10 (47)	0.09 (46)	-0.01 (50)

	Precipitation to discharge			
	DJF	**MAM**	**JJA**	**SON**
DJF	-0.06 (52)	0.18 (43)	0.25 (45)	0.09 (52)
MAM	-0.07 (48)	0.05 (52)	0.33 (32)	0.27 (44)
JJA	-0.06 (50)	0.19 (50)	-0.18 (51)	0.31 (40)
SON	0.29 (44)	-0.02 (50)	0.06 (51)	0.05 (52)

	Precipitation to to water temperature			
	DJF	**MAM**	**JJA**	**SON**
DJF	-0.04 (51)	-0.15 (48)	-0.26 (48)	0.05 (52)
MAM	0.24 (48)	0.36 (37)	-0.31 (36)	-0.11 (52)
JJA	-0.16 (50)	-0.06 (51)	0.13 (47)	-0.22 (47)
SON	0.14 (50)	0.04 (52)	-0.07 (51)	-0.06 (52)

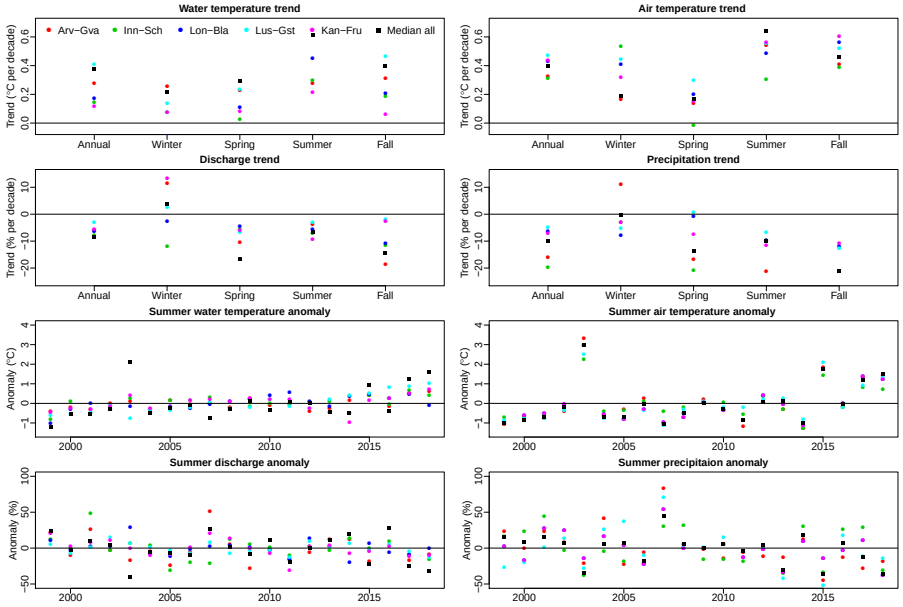

Figure S35. Top 2 rows: Annual and seasonal trends for water and air temperature and for discharge and precipitation over the 1999-2018 period. Trends for the five alpine catchments (colour dots, denoted as Arve in Geneva (Arv-Gva), Inn in S-Chanf (Inn-Sch), Lonza in Blatten (Lon-Bla), Lütschine in Gsteig (Lut-Gst) and Kander in Frutigen (Kan-Fru)) and median for all 52 catchments (black square). Bottom 2 rows : Summer anomalies for the same four variables, five catchments and period as on top. Median of the 52 catchments is also shown by a black square.

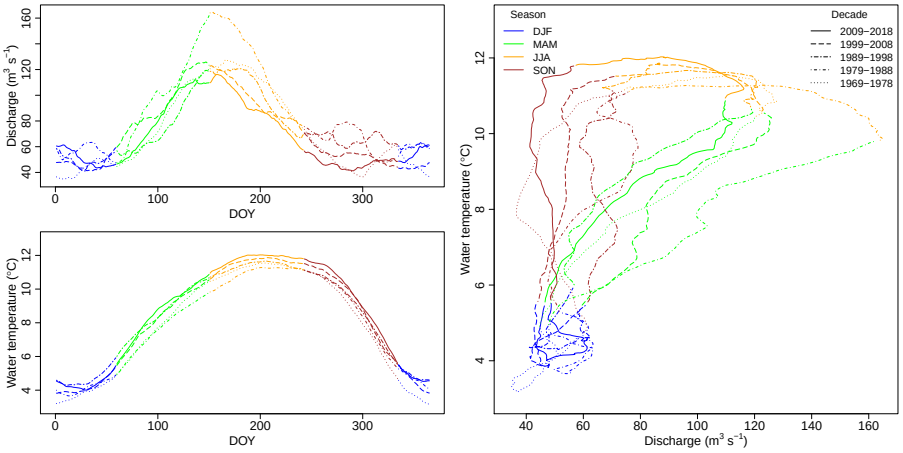

Figure S36. Left: Hydrological (top) and thermal (bottom) regimes per decade for the Arve River in Geneva averaged for each day of the year (DOY). Line types represent decades and colours the seasons. Right: Decadal temperature plotted against decadal discharge (both averaged for each day of the year).

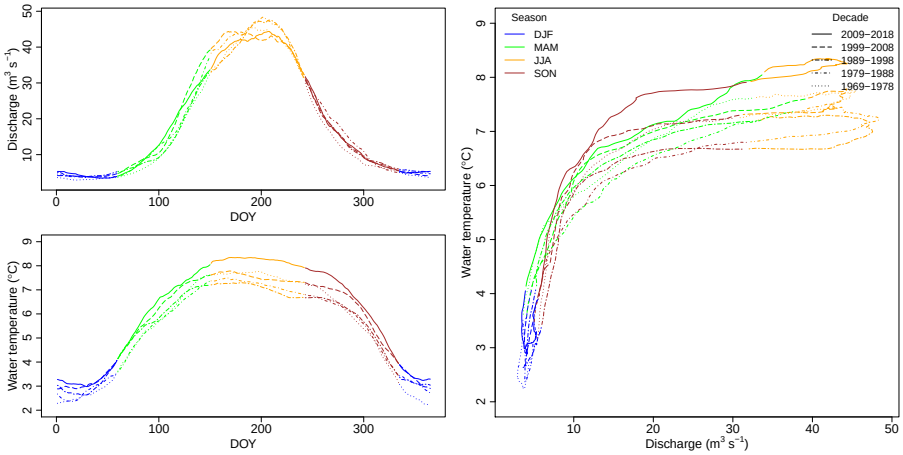

Figure S37. Left: Hydrological (top) and thermal (bottom) regimes per decade for the Lütschine River in Gsteig averaged for each day of the year (DOY). Line types represent decades and colours the seasons. Right: Decadal temperature plotted against decadal discharge (both averaged for each day of the year).

S2.4 Ecological indicators

This Section presents an additional Figure related to Section 4.5 of the main text. Figure S38 shows the summer runoff anomaly for the same catchments used in Figure 13 in the main text.

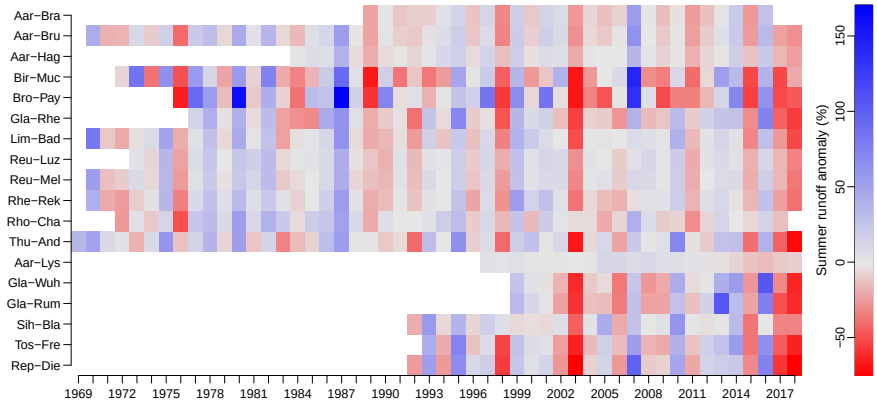

Figure S38. Summer relative runoff anomaly (with respect to the 1999-2018 period) for the catchments in which the 25 °C threshold is reached (see Figure 13 in main text).

References

Enfield, D., Mestas-Nunez, A., and Trimble, P.: The Atlantic multidecadal oscillation and its relation to rainfall and river flows in the continental US, Geophysical Research Letters, 28, 2077–2080, 2001.

GLAMOS: Swiss Glacier Mass Balance, release 2018, Glacier Monitoring Switzerland, doi:10.18750/massbalance.2018.r2018, 2018.

Hampel, F.: Robust Statistics: The Approach Based on Influence Functions, Probability and Statistics Series, Wiley, https://books.google.ch/books?id=KXWMNAAACAAJ, 1986.

Jones, P. D., Jonsson, T., and Wheeler, D.: Extension to the North Atlantic oscillation using early instrumental pressure observations from Gibraltar and south-west Iceland, International Journal of Climatology, 17, 1433–1450, https://doi.org/10.1002/(SICI)1097-0088(19971115)17:13<1433::AID-JOC203>3.0.CO;2-P, https://rmets.onlinelibrary.wiley.com/doi/abs/10.1002/%28SICI%291097-0088%2819971115%2917%3A13%3C1433%3A%3AAID-JOC203%3E3.0.CO%3B2-P, 1997.

Lehre Seip, K., Gron, O., and Wang, H.: The North Atlantic oscillations: Cycle times for the NAO, the AMO and the AMOC, Climate, 7, 43, https://doi.org/10.3390/cli7030043, 2019.

Magnusson, J., Gustafsson, D., Hüsler, F., and Jonas, T.: Assimilation of point SWE data into a distributed snow cover model comparing two contrasting methods, Water Resources Research, 50, 7816–7835, https://doi.org/10.1002/2014WR015302, https://agupubs.onlinelibrary.wiley.com/doi/abs/10.1002/2014WR015302, 2014.

Webb, B. W. and Nobilis, F.: Long-term changes in river temperature and the influence of climatic and hydrological factors, Hydrological Sciences Journal, 52, 74–85, https://doi.org/10.1623/hysj.52.1.74, 2007.